Biointerface Research in Applied Chemistry
Platinum Open Access Journal (ISSN: 2069-5837)

Article
Volume 12, Issue 1, 2022, 498 - 507
https://doi.org/10.33263/BRIAC121.498507

Selective Bromocyclization of 5-Amino-4-Alkenyl-1,2,4-Triazole-3-Thione

Maksym Fizer [1,*], Mikhailo Slivka [1], Oksana Fizer [1]

[1] Department of Organic Chemistry, Faculty of Chemistry, Uzhhorod National University, Fedinets', Str. 53/1, 88000, Uzhhorod, Ukraine
* Correspondence: max.fizer@uzhnu.edu.ua (M.F.);

Scopus Author ID 55823743600
Received: 9.03.2021; Revised: 10.04.2021; Accepted: 12.04.2021; Published: 20.04.2021

Abstract: Here, we present a study on the regioselectivity cyclization of 5-amino-4-alkenyl-1,2,4-triazole-3-thiones. The presence of various nucleophilic centers causes the possibility of cyclization of an alkenyl fragment on different heteroatoms and the formation of a few alternative structures. Elemental bromine was utilized as an electrophilic agent, and two 6-(bromomethyl)-6-R-5,6-dihydro[1,3]thiazolo[2,3-c][1,2,4]triazol-3-amine hydrobromide salts were obtained as the only products when taking reaction in chloroform, acetic acid, or acetonitrile. The 1H and 13C APT NMR spectra analysis proved the formation of the 1,3-thiazolinium ring upon cyclization reaction. DFT calculations at the ωB97X-D3/6-311G(d,p) level of theory were utilized to analyze molecular electrostatic potential, electron localization function, and Hirshfeld atomic partial charges the intermediate bromonium cation. These theoretical calculations explain the experimentally observed regioselectivity.

Keywords: 1,2,4-triazole; cyclization; regioselectivity; NMR; DFT; electron localization function.

1. Introduction

One of the powerful methods for designing condensed heterocycles is electrophilic cyclization, widely used in modern synthetic organic chemistry [1–5]. In previous works, we presented a synthetic strategy for obtaining positive charge fused triazoles [6,7]. Moreover, we have established that the bromo-cyclization of 5-alkenylamino-4-alkenyl-1,2,4-triazole-3-thione selectively leads to the condensed [1,3]thiazolo[2,3-c][1,2,4]triazole systems [8–10]. However, Ernst et al. have described methods for obtaining imidazo[2,1-c][1,2,4]triazoline-3-thiones and [1,3]thiazolo[2,3-c][l,2,4]triazoles via the bromination of 4-methallyl-substituted 1,2,4-triazole-3-thiones [11]. The authors have managed to obtain different products by variation of the nucleophilicity of the core 5-amino-1,2,4-triazole-3-thione system. Here we have to clarify that in our previous works, only 5-R-amino-substituted triazoles were utilized. Consequently, bearing in mind the exclusion of possible steric hindrance of the exocyclic amino group nitrogen atom, we have synthesized 4-allyl-5-amino-1,2,4-triazole-3-thione 2a and 5-amino-4-methallyl-1,2,4-triazole-3-thione 2b. The regioselectivity of the bromination of these two compounds in chloroform, acetonitrile, and acetic acid, was investigated.

2. Materials and Methods

All reagents and solvents were purchased from Sigma-Aldrich, Acros Organics, or Sfera Sim companies and were used without additional purification. Varian VXR-300 instrument was used to record NMR spectra in deuterated dimethyl sulfoxide (DMSO–d6). Tetramethylsilane (TMS) was used as an internal standard. Theoretical DFT calculations were performed with the Xeon 12 core workstation with 64 GB of RAM.

The synthesis of 1-alkenyl-2,5-dithioureas 1a and 1b was performed starting from thiosemicarbazide and allyl isothiocyanate or methallyl isothiocyanate [12], respectively, via the known procedure [13].

2.1. 1-Allyl-2,5-dithiourea (1a).

The yield is 58%; mp 180–181 °C; ^{1}H NMR (300 MHz, DMSO-d6), δ (ppm): 9.38 (s, 1H, NH_2); 8.20 (br.s, 1H, NH-CH_2), 8.07 (br.s, 1H, NH), 7.32 (br.s, 1H, NH), 5.86 (m, 1H, -CH=), 5.07 (dd, *J* = 25.8, 13.6 Hz, 2H, =CH_2), 4.08 (t, *J* = 5.0 Hz, 2H, NH-CH_2); the elemental analysis: found: C, 31.61; H, 5.52; N, 29.21; S 33.46%; calc. for $C_5H_{10}N_4S_2$: C, 31.56; H, 5.30; N, 29.44; S, 33.70%.

2.2. 1-Methallyl-2,5-dithiourea (1b).

The yield is 70%; mp 195–196 °C; ^{1}H NMR (300 MHz, DMSO-d6), δ (ppm): 9.36 (s, 1H, NH_2), 8.05 (br.s, 1H, NH), 7.94 (t, J = 5.2 Hz, 1H, NH-CH_2), 7.28 (br.s, 1H, NH), 4.78 (s, 1H, =CH_2), 4.74 (s, 1H, =CH_2), 4.02 (d, J = 3.5 Hz, 2H, NH-CH_2), 1.66 (s, 3H, CH_3); the elemental analysis: found: C, 35.42; H, 6.09; N, 27.21; S 31.05%; calc. for $C_6H_{12}N_4S_2$: C, 35.27; H, 5.92; N, 27.42; S, 31.39%.

The synthesis of 4-alkenyl-5-amino-1,2,4-triazole-3-thiones 2a and 2b was performed starting from 1-alkenyl-2,5-dithioureas 1a and 1b, respectively, via the basic-catalyzed cyclization following the known procedure [10, 13].

2.3. 4-Allyl-5-amino-2,4-dihydro-3H-1,2,4-triazole-3-thione (2a).

The yield is 78%; mp 124–126 °C; ^{1}H NMR (300 MHz, DMSO-d6), δ (ppm): 6.15 (s, 2H, NH_2), 5.80 (m, 1H, –CH=), 5.10 (dd, *J* = 28.0, 13.3 Hz, 2H, =CH_2), 4.47 (d, J = 5.1 Hz, 2H, NCH_2); the elemental analysis: found: C, 38.32; H, 5.42; N, 35.61; S 20.22%; calc. for $C_5H_8N_4S$: C, 38.44; H, 5.16; N, 35.87; S, 20.53%.

2.4. 5-Amino-4-methallyl-2,4-dihydro-3H-1,2,4-triazole-3-thione (2b).

The yield is 80%; mp 158–159 °C; ^{1}H NMR (300 MHz, DMSO-d6), δ (ppm): 6.08 (s, 2H, NH_2), 4.81 (s, 1H, =CH_2), 4.44 (s, 1H, =CH_2), 4.39 (s, 2H, NCH_2), 1.68 (s, 3H, CH_3); the elemental analysis: found: C, 42.22; H, 6.08; N, 32.77; S 18.65%; calc. for $C_6H_{10}N_4S$: C, 42.33; H, 5.92; N, 32.91; S, 18.84%.

2.5. The general procedure of bromo-cyclization.

To a solution of the corresponding 4-alkenyl-5-amino-1,2,4-triazole-3-thione (0.02 mol) in a solvent (50 ml), a solution of bromine (0.02 mol) in 20 ml of a solvent was added for 30 min with constant stirring. The mixture was further stirred for another hour. The target

product was precipitated, filtered, washed with acetone, and recrystallized from ethanol. As solvents, we used chloroform, acetonitrile, and acetic acid.

2.6. 6-(Bromomethyl)-5,6-dihydro[1,3]thiazolo[2,3-c][1,2,4]triazol-3-amine hydrobromide (3a).

The yield is 78% (from chloroform), 77% (from acetonitrile), 65% (from acetic acid) ; mp 180–181 °C (recrystallized from ethanol); ^{1}H NMR (300 MHz, DMSO-d6), δ (ppm): 8.38 (br. s, 2H, NH_2), 5.01–4.72 (m, 1H, SCH), 4.19 (ddd, *J* = 15.2, 11.5, 5.5 Hz, 2H, NCH_2), 3.88–3.68 (m, 2H, CH_2Br), 3.85 (very br. s, water signal that overlapped with HBr proton); ^{13}C APT NMR (75 MHz, DMSO-d6), δ (ppm): 154.3 (C), 149.4 (C), 48.6 (CH_2N), 45.9 (CHS), 36.8 (CH_2Br); the elemental analysis: found: C, 18.92; H, 2.80; N, 17.56; S 10.02%; calc. for $C_5H_8Br_2N_4S$: C, 19.00; H, 2.55; N, 17.73; S, 10.15%.

2.7. 6-(Bromomethyl)-6-methyl-5,6-dihydro[1,3]thiazolo[2,3-c][1,2,4]triazol-3-amine hydrobromide (3b).

The yield is 68% (from chloroform), 69% (from acetonitrile), 59% (from acetic acid); mp 188–189 °C; ^{1}H NMR (300 MHz, DMSO-d6), δ (ppm): 6.54 (br. s, 2H, NH_2), 3.98 (dd, *J* = 68.3, 11.5 Hz, 2H, NCH_2), 3.88 (s, 2H, CH_2Br), 3.49 (very br. s, water signal that overlapped with HBr proton), 1.75 (s, 3H, CH_3); ^{13}C APT NMR (75 MHz, DMSO-d6), δ 155.5 (C), 143.0 (C), 59.06 (CH_2N), 54.9 (CS), 38.6 (CH_2Br), 30.1 (CH_3); the elemental analysis: found: C, 21.59; H, 3.20; N, 16.71; S 9.56%; calc. for $C_6H_{10}Br_2N_4S$: C, 21.83; H, 3.05; N, 16.98; S, 9.72%.

Density functional theory calculations were performed in the ORCA 4.2 package [14, 15] with the ωB97X-D3 [16–18] functional and 6-311G(d,p) basis set [19]. The "Resolution of identity" [20-22] and "Chain-of-spheres" [23–25] techniques were utilized to speed up all calculations. Visualization of isosurfaces was performed with VMD [26] and ChimeraX [27,28] packages.

3. Results and Discussion

Synthesis of 4-alkenyl-1,2,4-triazoles 2a,b was performed according to Scheme 1. The reaction of thiosemicarbazide with allyl isothiocyanate or methallyl isothiocyanate leads to corresponding 1-alkenyl-2,5-dithioureas 1a,b.

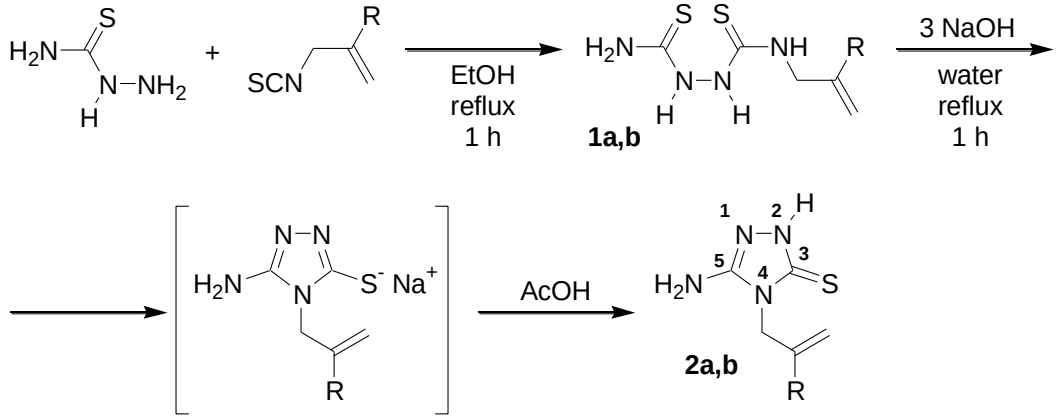

R = H (**a**), CH_3 (**b**).

Scheme 1. Synthesis of 4-alkenyl-5-amino-1,2,4-triazole-3-thiones 2a,b. Numeration in the triazole ring is presented.

Further cyclization of 1a,b in a 25% water solution of sodium hydroxide under heating leads to the 4-alkenyl-5-amino-1,2,4-triazole-3-thiolate sodium salts. Direct acidification of the reaction mixture leads to the precipitation of target 4-alkenyl-5-amino-1,2,4-triazole-3-thiones 2a,b.

The synthesized triazoles 2a,b contain numerous nucleophilic centers, namely, alkenyl double bond, the thione sulfur atom, two pyridine-type endocyclic nitrogen atoms in positions 1 and 2 of the triazole ring, and the exocyclic amino group nitrogen connected with carbon 5. Nitrogen in position 4 of the ring cannot be considered a nucleophilic center because it is pyrrole-type nitrogen. Its electron pair is involved in the triazole ring aromatic conjugation. All these present nucleophilic centers make these triazoles interesting objects for investigating the regio-direction of the interaction with electrophilic reagents. In the current work, elemental bromine was selected as an electrophilic agent.

The formation of bromine-sulfur/nitrogen charge-transfer complexes is described in the literature [29–32]. Possible ways of interaction of bromine with heteroatom-nucleophilic centers in thiones 2a,b are presented in Figure 1a. Moreover, taking into account thione-thiol tautomerism, the alternative structures are possible according to Figure 1b. Here we have to clarify that such complexes are not thermodynamically stable; Br–Br S and Br–Br N bonds can be broken easily.

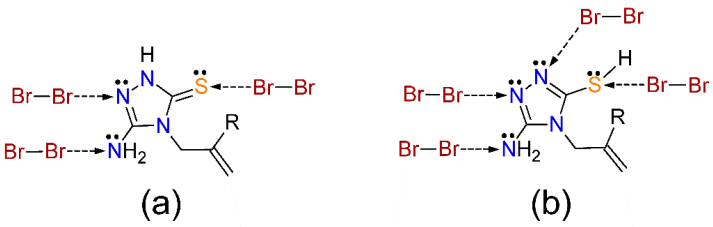

Figure 1. Possible Br–Br S and Br–Br N complexes of triazoles 2a,b with bromine: (a) in thione form; (b) in thiol form.

Conversely, the interaction of bromine molecule with the double bond leads to the π-complexes 2'a,b, which liberate the bromide anions and form bromonium cations 2" a,b (see Scheme 2). There must be considered five possible further transformations of 2" a,b. An attack of a lone electron pair of the nucleophilic sulfur atom on the bromonium cation can lead to the annulation of 1,3-thiazole (3a,b) or 1,3-thiazine (3'a,b) cycles. Interaction of bromonium cation with bromide anion leads to the vicinal dibromide 3" a,b. Finally, an attack of a lone electron pair of the exocyclic amino group on the bromonium cation can lead to the annulation of 1,3-imidazole (3"'a,b) or pyrimidine (3""a,b) cycles.

Analysis of NMR data testifies the selective formation of 3a,b products. For example, the alternative structures 3"'a,b and 3""a,b have to be discarded as the ^{1}H NMR spectra contain only one signal that according to chemical shift can be related to NC-H, namely the split doublet of doublets at 4.19 ppm (ddd, J = 15.2, 11.5, 5.5 Hz) in the case of 3a, and the split doublet of doublets at 3.98 ppm (dd, J = 68.3, 11.5 Hz, 2H, NCH_2) in the case of 3b.

The ^{1}H NMR spectrum of the 2a cyclization product contains a multiplet at 4.86 ppm related to a methine group connected with two methylene groups. According to the literature data [9,10], a multiplet with such chemical shift corresponds to HC–S group. In the case of 3"a,b, the NCH_2 and CH_2Br groups in the linear 2,3-dibromopropyl chain would be shown as a doublet. However, the NCH_2 group signal is split considerably, which testifies to the endocyclic nature of the NCH_2 group, and axial- and equatorial-hydrogen atoms give different signals. The signal of the CH_2Br group is a multiplet at 3.68–3.88 ppm instead of an expected

doublet. This can be explained by the chiral HC–S group and numerous conformers due to hindered rotation in the CH_2Br group. The 3'a,b, and 3"'a,b forms with six-membered cycles can be excluded due to the absence of considerable splitting of the signals analogously to the above-discussed endocyclic NCH_2 splitting.

The ^{13}C APT NMR spectra analysis also confirms the formation of the 3a,b structures – the downfield methylene group signals related to CH_2Br groups. In the case of the 3a compound, the positive signal at 45.9 ppm corresponds to an HC–S group, whereas, in 3b, the negative signal of C–S carbon is located at 54.9 ppm. The acidic proton assignment to the first nitrogen atom of the triazole ring is based on literature data, where it was shown that triazolium salts contain protons near that nitrogen [33,34].

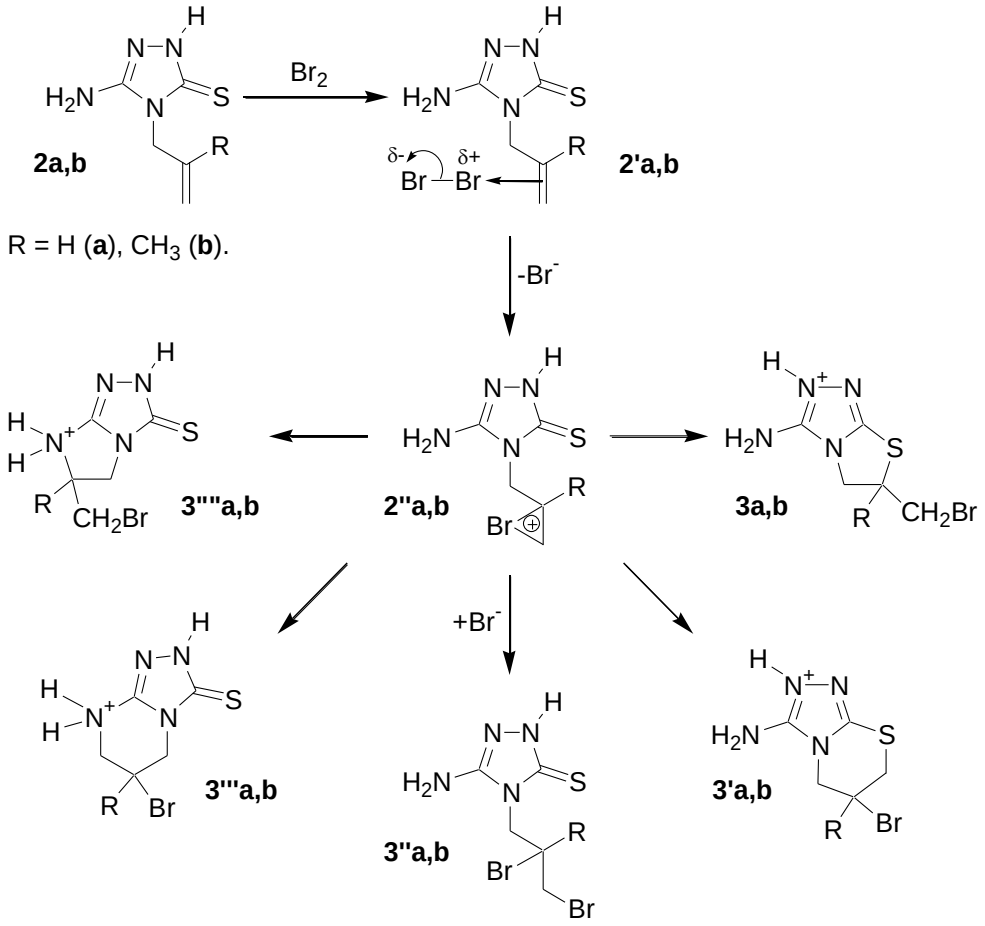

Scheme 2. Possible mechanisms of bromination of triazoles 2a,b.

To explain the observed regioselectivity of bromination of 2a,b, we have calculated various reactivity descriptors via a DFT method. At first, the gas-phase geometry of the four most plausible structures of cation 2"a was optimized at ωB97X-D3/6-311G(d,p) level of theory (Figure 2). We considered thione form with the bromine atom attached from the amino group side (Figure 2a) and the sulfur atom side (Figure 2b). Similarly, the thiol tautomers with the bromine atom attached from the amino group side (Figure 2c) and the sulfur atom side (Figure 2d) were considered. The electrostatic potential (ESP) isosurface was generated with the Multiwfn program [35] via the Libreta algorithm [36] using the electron density generated with the ωB97X-D3/6-311G(d,p) method in gas-phase, chloroform, and acetonitrile medium; however, for clarity, only the gas-phase calculation shown in Figure 2. Red areas are related to low values of ESP (30–70 kcal/mol), whereas the green and blue regions correspond to medium (70–130 kcal/mol) and high (130–170 kcal/mol) ESP values, respectively. As can be seen, the

lowest values of ESP are located over the exocyclic sulfur atom, exocyclic amino group nitrogen, and pyridinium-type endocyclic nitrogen atoms.

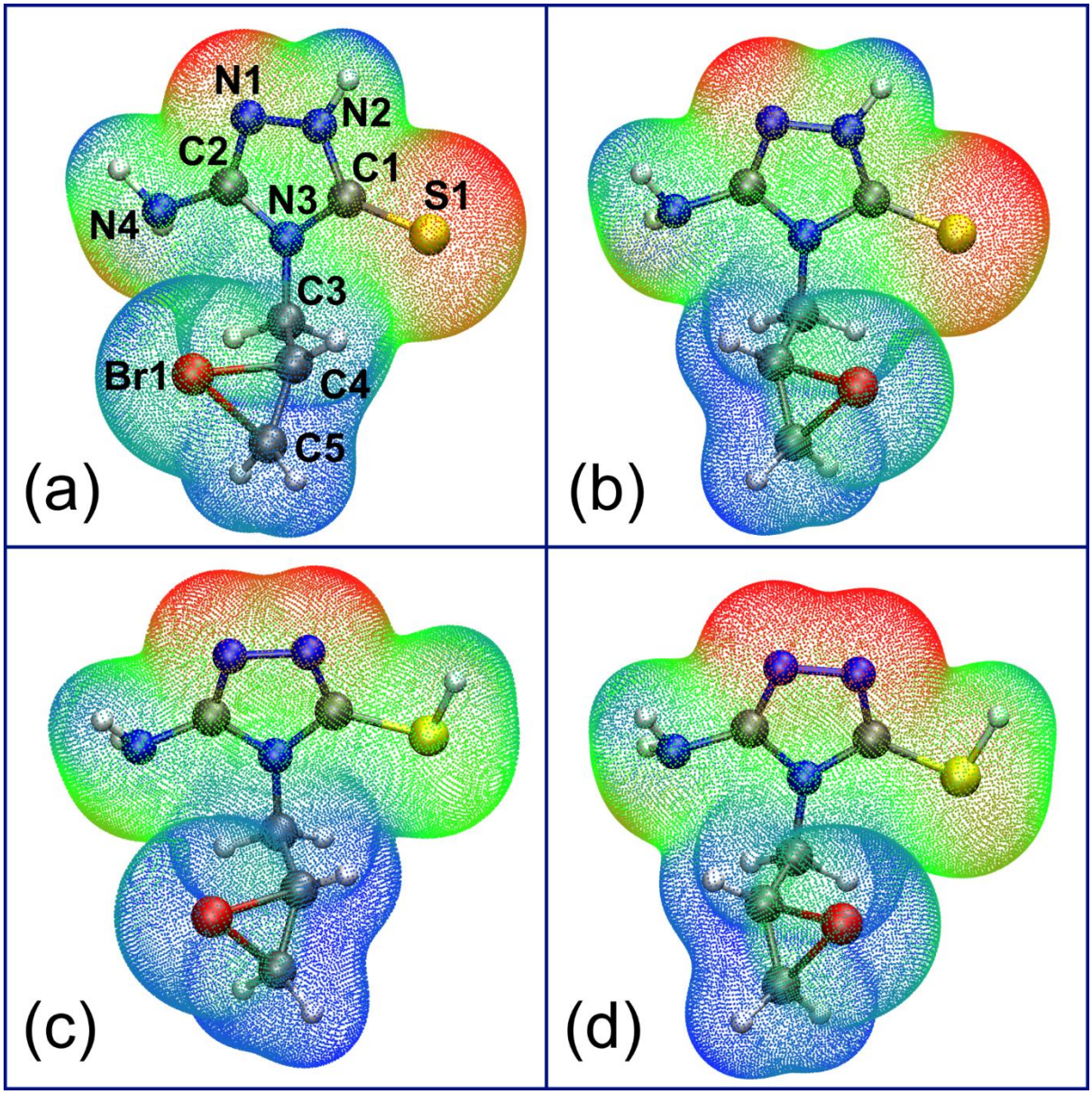

Figure 2. ESP isosurface of four structures of bromonium cation 2"a.

The electron localization function (ELF) isosurface with an isovalue of 0.89 was also analyzed as a regioselectivity descriptor. A larger ELF isosurface corresponds to a higher probability of electron pairs' location and higher nucleophilicity. In Figure 3, the ELFs of the four forms of cation 2"a are shown. Hydrogen atoms are represented as large green domains, the large blue blobs correspond to lone pair domains, and covalent bond domains are presented as relatively small yellow areas. Atom center domains are shown as red balls. Taking into account the areas of lone pair domains, the heteroatoms can be ordered according to their nucleophilicity as follows: (a) the S1 sulfur atom is the most nucleophilic; (b) N1 and N2 (only in the case of thiols c, d) nitrogen atoms are slightly less nucleophilic; (c) bromine atom of the bromonium cycle; (d) the exocyclic amino group nitrogen atom shows the lowest nucleophilicity. A notable decrease of the ELF near the sulfur atom in thiol forms c, d is caused by the sharing of S1 electron density with the attached hydrogen atom.

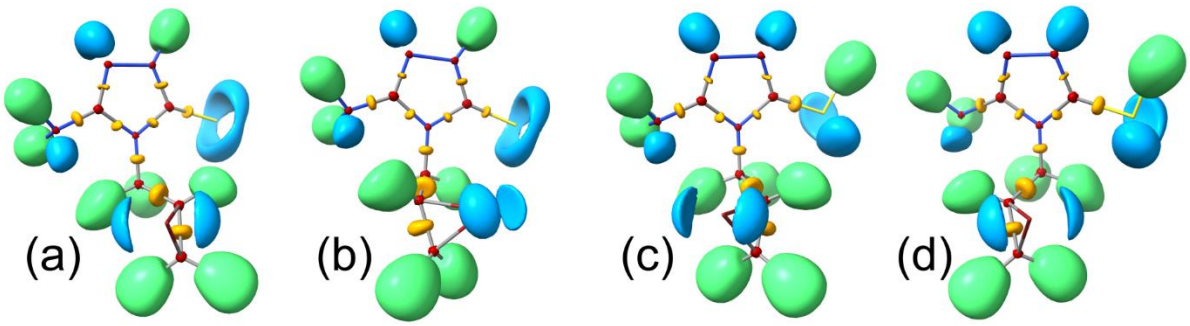

Figure 3. ELF isosurface of four structures of bromonium cation 2"a.

For a more precise grading of the above-mentioned nucleophilic centers, the Hirshfeld [35–38] atomic partial charges were calculated. The choice was dictated by the well-known use of Hirshfeld charges in reactivity prediction [39, 40]. As can be seen from Table 1, for all studied geometries and in all phases, the C4 atom is more electrophilic than C5, which explains the preferred form of the five-membered cycle. In turn, thione forms a and b are characterized with a lower charge on the sulfur atom, which testifies the preferred cyclization on the S1 atom. However, in thiol forms c and d, N4 nitrogen has a lower charge than the S1 atom, which predicts the formation of imidazole systems 3""a,b (Scheme 2), contradicting the experimental data.

Table 1. Hirshfeld atomic partial charges on S1, N4, C4, and C5 atoms in a-d forms of 2"a cation.

Cation geometry	Phase	Atom			
		S1	N4	C4	C5
a	gas	–0.2876	–0.1841	0.1067	0.0815
	chloroform	–0.3724	–0.1799	0.1111	0.0941
	acetonitrile	–0.3959	–0.1780	0.1120	0.0976
b	gas	–0.3036	–0.1807	0.1039	0.0786
	chloroform	–0.3885	–0.1739	0.1128	0.0933
	acetonitrile	–0.4126	–0.1712	0.1158	0.0978
c	gas	–0.0117	–0.1971	0.1057	0.0811
	chloroform	–0.0117	–0.1894	0.1119	0.0952
	acetonitrile	–0.0097	–0.1867	0.1137	0.0995
d	gas	–0.0201	–0.1836	0.1033	0.0821
	chloroform	–0.0207	–0.1752	0.1106	0.0968
	acetonitrile	–0.0193	–0.1721	0.1129	0.1013

To resolve this contradiction, we have to compare the relative Gibbs free energies of the a-d forms. The data calculated at the ωB97X-D3/6-311G(d,p) level of theory is summarized in Table 2. Obviously, the quantity of the thiol forms of c and d is negligible due to the thione form's much higher stability.

Table 2. Relative Gibbs free energy (kcal/mol) at 298.15 K, and Boltzman distribution (%) of forms of cation 2"a.

Phase	Cation 2"a form	Relative Gibbs free energy, kcal/mol	Boltzmann distribution, %
Gas	a	0.00	83.78
	b	0.97	16.22
	c	18.94	1.09×10^{-12}
	d	18.51	2.27×10^{-12}
Chloroform	a	0.00	52.72
	b	0.06	47.28
	c	15.77	1.46×10^{-10}
	d	15.83	1.32×10^{-10}
Acetonitrile	a	0.23	40.42
	b	0.00	59.58
	c	15.06	5.47×10^{-10}
	d	15.25	3.96×10^{-10}

4. Conclusions

The syntheses of new 5-amino-4-alkenyl-1,2,4-triazole-3-thiones were performed. The reaction of these thiones with elemental bromine in chloroform, acetic acid, or acetonitrile selectively leads to the formation of 6-(bromomethyl)-6-R-5,6-dihydro[1,3]thiazolo[2,3-c][1,2,4]triazol-3-amine hydrobromide salts. The detailed analysis of ^{1}H and ^{13}C APT NMR spectra were used for the determination of the structure. A few alternative pathways have been proposed in this study; however, investigation of molecular electrostatic potential, electron localization function, and Hirshfeld atomic partial charges of the intermediate bromonium cation clearly shows the preferred attack of the more nucleophilic sulfur atom and consequent formation of the 1,3-thiazoline cycle.

Funding

This study was partially supported by the Ministry of Education and Science of Ukraine (State Budget Projects 0119U100232 and 0120U100431) and by the Slovak Academic Information Agency (National Scholarship Programme of the Slovak Republic, Grants ID 25718 and 30750).

Acknowledgments

This research has no acknowledgment.

Conflicts of Interest

The authors declare no conflict of interest.

References

1. Kim, D.G.; Vershinina, E.A.e.; Sharutin, V.V. Synthesis, transformations and halocyclization of 8-(Prop-2-ynylsulfanyl)quinoline and 8-(2-Bromoprop-2-enylsulfanyl)quinoline. *Journal of Sulfur Chemistry* **2020**, *41*, 71-81, https://doi.org/10.1080/17415993.2019.1677660.
2. Danyliuk, I.Y.; Vas'kevich, R.I.; Vas'kevich, A.I.; Rusanov, E.B.; Vovk, M.V. Sulfanyl chloride induced heterocyclization of N-(pyrazolyl)styrylacetamides. *Phosphorus, Sulfur, and Silicon and the Related Elements* **2019**, *194*, 156-162, https://doi.org/10.1080/10426507.2018.1528257.
3. Danyliuk, I.Y.; Vas'kevich, R.I.; Vas'kevich, A.I.; Vovk, M.V. Hydrogenated benzazepines: recent advances in the synthesis and study of biological activity. *Chemistry of Heterocyclic Compounds* **2019**, *55*, 802-814, https://doi.org/10.1007/s10593-019-02540-3.
4. Volkova, Y.A.; Averina, E.B.; Vasilenko, D.A.; Sedenkova, K.N.; Grishin, Y.K.; Bruheim, P.; Kuznetsova, T.S.; Zefirov, N.S. Unexpected Heterocyclization of Electrophilic Alkenes by Tetranitromethane in the Presence of Triethylamine. Synthesis of 5-Nitroisoxazoles. *The Journal of Organic Chemistry* **2019**, *84*, 3192-3200, https://doi.org/10.1021/acs.joc.8b03086.
5. D'hollander, A.; Peilleron, L.; Grayfer, T.; Cariou, K. Halonium-induced polyene cyclizations. *Synthesis* **2019**, *51*, 1753-1769, https://doi.org/10.1055/s-0037-1612254.
6. Fizer, M.M.; Slivka, M.V.; Lendel, V.G. New method of synthesis of 3,5,6,7-tetrahydro-[1,2,4]triazolo[1,5-a]pyrimidine-2(1H)-thione. *Chemistry of Heterocyclic Compounds* **2013**, *49*, 1243-1245, https://doi.org/10.1007/s10593-013-1369-z.
7. Korol, N.; Slivka, M.; Fizer, M.; Baumer, V.; Lendel, V. Halo-heterocyclization of butenyl(prenyl)thioethers of 4,5-diphenyl-1,2,4-triazol-3-thiole into triazolo[5,1-b] [1,3]thiazinium systems: experimental and theoretical evolution. *Monatshefte für Chemie - Chemical Monthly* **2020**, *151*, 191-198, https://doi.org/10.1007/s00706-019-02545-w.

8. Fizer, M.; Slivka, M.; Rusanov, E.; Turov, A.; Lendel, V. [1,3]Thiazolo[2′,3′:3,4][1,2,4]triazolo[1,5-a]pyrimidines – A New Heterocyclic System Accessed via Bromocyclization. *J. Heterocycl. Chem.* **2015**, *52*, 949-952, https://doi.org/10.1002/jhet.2073.
9. Khripak, S.M.; Slivka, M.V.; Vilkov, R.V.; Usenko, R.N.; Lendel, V.G. Regioselectivity of the monohalogenation of 4-allyl-3-allylamino-1,2,4-triazole-5-thione. *Chemistry of Heterocyclic Compounds* **2007**, *43*, 781-785, https://doi.org/10.1007/s10593-007-0126-6.
10. Fizer, M.M.; Slivka, M.V.; Lendel, V.G. Peculiarities of 4-methallyl-5-methallylamino-1,2,4-triazole-3-thione halogenation. *Chemistry of Heterocyclic Compounds* **2019**, *55*, 478-480, https://doi.org/10.1007/s10593-019-02484-8.
11. Ernst, S.; Jelonek, S.; Sieler, J.; Schulze, K. 4-Methallyl substituted 1,2,4-triazoline-3-thiones as a source of N-bridgehead heterocycles. *Tetrahedron* **1996**, *52*, 791-798, https://doi.org/10.1016/0040-4020(95)01038-6.
12. Fizer, M. Methallyl isothiocyanate. *Synlett* **2013**, *24*, 2019-2020, https://doi.org/10.1055/s-0033-1339703.
13. Altland, H.W.; Graham, P.A. Cyclization of 1-substituted-3-thiosemicarbazides to triazole derivatives under alkaline conditions. *J. Heterocycl. Chem.* **1978**, *15*, 377-384, https://doi.org/10.1002/jhet.5570150305.
14. Neese, F. Software update: the ORCA program system, version 4.0. *WIREs Computational Molecular Science* **2018**, *8*, e1327, https://doi.org/10.1002/wcms.1327.
15. Neese, F.; Wennmohs, F.; Becker, U.; Riplinger, C. The ORCA quantum chemistry program package. *The Journal of Chemical Physics* **2020**, *152*, 224108, https://doi.org/10.1063/5.0004608.
16. Lin, Y.-S.; Li, G.-D.; Mao, S.-P.; Chai, J.-D. Long-Range Corrected Hybrid Density Functionals with Improved Dispersion Corrections. *J. Chem. Theory Comput.* **2013**, *9*, 263-272, https://doi.org/10.1021/ct300715s.
17. Baumgärtner, K.; Hoffmann, M.; Rominger, F.; Elbert, S.M.; Dreuw, A.; Mastalerz, M. Homoconjugation and intramolecular charge transfer in extended aromatic triptycenes with different π-planes. *J. Org. Chem.* **2020**, *85*, 15256–15272, https://dx.doi.org/10.1021/acs.joc.0c02100.
18. Dakota Folmsbee Geoffrey Hutchison. Assessing conformer energies using electronic structure and machine learning methods. *Int. J. Quantum Chem.* **2021**, *121*, e26381, https://doi.org/10.1002/qua.26381.
19. Deraet, X.; Woller, T.; Van Lommel, R.; De Proft, F.; Verniest, G.; Alonso, M. A Benchmark of density functional approximations for thermochemistry and kinetics of hydride reductions of cyclohexanones. *ChemistryOpen* **2019**, *8*, 788–806, https://doi.org/10.1002/open.201900085.
20. Kussmann, J.; Laqua, H.; Ochsenfeld, C. Highly efficient resolution-of-identity density functional theory calculations on central and graphics processing units. *J. Chem. Theory Comput.* **2021**, *17*, 1512–1521, https://doi.org/10.1021/acs.jctc.0c01252.
21. Dou, W.; Chen, M.; Takeshita, T.Y.; Baer, R.; Neuhauser, D.; Rabani, E. Range-separated stochastic resolution of identity: Formulation and application to second-order Green's function theory. *J. Chem. Phys.* **2020**, *153*, 074113, https://doi.org/10.1063/5.0015177.
22. Lin, P.; Ren, X.; He, L. Accuracy of localized resolution of the identity in periodic hybrid functional calculations with numerical atomic orbitals. *J. Phys. Chem. Lett.* **2020**, *11*, 3082–3088, https://doi.org/10.1021/acs.jpclett.0c00481.
23. Neese, F.; Wennmohs, F.; Hansen, A.; Becker,U. Efficient, approximate and parallel Hartree-Fock and hybrid DFT calculations. A 'chain-of-spheres' algorithm for the Hartree-Fock exchange. *Chem. Phys.* **2009**, *356*, 98–109, https://doi.org/10.1016/j.chemphys.2008.10.036.
24. Shirazi, R.G.; Pantazis, D.A.; Neese, F. Performance of density functional theory and orbital-optimised second-order perturbation theory methods for geometries and singlet–triplet state splittings of aryl-carbenes. *Mol. Phys.* **2020**, *118*, e1764644, https://doi.org/10.1080/00268976.2020.1764644.
25. Maier, T.M.; Ikabata, Y.; Nakai, H. Efficient semi-numerical implementation of relativistic exact exchange within the infinite-order two-component method using a modified chain-of-spheres method. *J. Chem. Theory Comput.* **2019**, *15*, 4745–4763, https://doi.org/10.1021/acs.jctc.9b00228.
26. Humphrey, W.; Dalke, A.; Schulten, K. VMD - visual molecular dynamics. *J. Molec. Graphics* **1996**, *14*, 33–38, https://doi.org/10.1016/0263-7855(96)00018-5.
27. Goddard, T.D.; Huang, C.C.; Meng, E.C.; Pettersen, E.F.; Couch, G.S.; Morris, J.H.; Ferrin, T.E. UCSF ChimeraX: Meeting modern challenges in visualization and analysis. *Protein Sci.* **2018**, *27*, 14–25, https://doi.org/10.1002/pro.3235.
28. Pettersen, E.F.; Goddard, T.D., Huang, C.C.; Meng, E.C.; Couch, G.S.; Croll, T.I.; Morris, J.H.; Ferrin, T.E. UCSF ChimeraX: Structure visualization for researchers, educators, and developers. *Protein Sci.* **2021**, *30*, 70–82, https://doi.org/10.1002/pro.3943.

29. de Faria, D.L.A.; Gonçalves, N.S.; Santos, P.S. Vibrational spectra of iodine and bromine thiourea complexes. *Spectrochim. Acta A* **1989**, *45*, 643–647, https://doi.org/10.1016/0584-8539(89)80172-2.
30. Vaughan, G.B.M.; Mora, A.J.; Fitch, A.N.; Gates, P.N.; Muir, A.S. A high resolution powder X-ray diffraction study of the products of reaction of dimethyl sulfide with bromine; crystal and molecular structures of $(CH_3)_2SBr_n$ (n = 2, 2.5 or 4). *J. Chem. Soc., Dalton Trans.* **1999**, *1999*, 79–84, https://doi.org/10.1039/A805942J.
31. Pejic, M.; Popp, S.; Bolte, M.; Wagner, M.; Lerne, H.-W. Functionalized pyrazoles as agents in C–C cross-coupling reactions. *Z. Naturforsch. B* **2014**, *69b*, 83–97, https://doi.org/10.5560/znb.2014-3224.
32. Nemec, V.; Lisac, K.; Stilinović, V.; Cinčić, D. Inorganic bromine in organic molecular crystals: Database survey and four case studies. *J. Mol. Struct.* **2017**, *1128*, 400–409, https://doi.org/10.1016/j.molstruc.2016.08.034.
33. Fizer, M.; Slivka, M.; Mariychuk, R.; Baumer, V.; Lendel, V. 3-Methylthio-4-phenyl-5-phenylamino-1,2,4-triazole hexabromotellurate: x-ray and computational study. *J. Mol. Struct.* **2018**, *1161*, 226–236, https://doi.org/10.1016/j.molstruc.2018.02.054.
34. Fizer, M.; Slivka, M.; Sidey, V.; Baumer, V.; Mariychuk, R. *J. Mol. Struct.* **2021**, *1235*, 130227, https://doi.org/10.1016/j.molstruc.2021.130227.
35. Lu, T.; Chen, F. Multiwfn: a multifunctional wavefunction analyzer. *J. Comput. Chem.* **2012**, *33*, 580–592, https://doi.org/10.1002/jcc.22885.
36. Zhang, J. Libreta: computerized optimization and code synthesis for electron repulsion integral evaluation. *J. Chem. Theory Comput.* **2018**, *14*, 572–587, https://doi.org/10.1021/acs.jctc.7b00788.
37. Hirshfeld, F.L. Bonded-atom fragments for describing molecular charge densities. *Theor. Chim. Acta* **1977**, *44*, 129–138, https://doi.org/10.1007/BF00549096.
38. Fizer, O.; Fizer, M.; Sidey, V.; Studenyak, Y.; Mariychuk, R. Benchmark of different charges for prediction of the partitioning coefficient through the hydrophilic/lipophilic index. *J. Mol. Model.* **2018**, *24*, 141, https://doi.org/10.1007/s00894-018-3692-x.
39. Kut, M.; Fizer, V.; Onysko, M.; Lendel, V. Reactions of N-alkenylthioureas with p-alkoxyphenyltelluriumtrichlorides. *J. Heterocyclic Chem.* **2018**, *55*, 2284–2290, https://doi.org/10.1002/jhet.3281.
40. Bandyopadhyay, P.; Raya, S.; Seikh, M.M. Unraveling the regioselectivity of odd electron halogen bond formation using electrophilicity index and chemical hardness parameters. *Phys. Chem. Chem. Phys.* **2019**, *21*, 26580–26590, https://doi.org/10.1039/C9CP05374C.